Prenatal Exposure to the Environmental Obesogen Tributyltin Predisposes Multipotent Stem Cells to Become Adipocytes

Séverine Kirchner, Tiffany Kieu, Connie Chow, Stephanie Casey, and Bruce Blumberg

Department of Developmental and Cell Biology, University of California, Irvine, California 92697-2300

The environmental obesogen hypothesis proposes that pre- and postnatal exposure to environmental chemicals contributes to adipogenesis and the development of obesity. Tributyltin (TBT) is an agonist of both retinoid X receptor (RXR) and peroxisome proliferator-activated receptor γ (PPARγ). Activation of these receptors can elevate adipose mass in adult mice exposed to the chemical *in utero*. Here we show that TBT sensitizes human and mouse multipotent stromal stem cells derived from white adipose tissue [adipose-derived stromal stem cells (ADSCs)] to undergo adipogenesis. *In vitro* exposure to TBT, or the PPARγ activator rosiglitazone increases adipogenesis, cellular lipid content, and expression of adipogenic genes. The adipogenic effects of TBT and rosiglitazone were blocked by the addition of PPARγ antagonists, suggesting that activation of PPARγ mediates the effect of both compounds on adipogenesis. ADSCs from mice exposed to TBT *in utero* showed increased adipogenic capacity and reduced osteogenic capacity with enhanced lipid accumulation in response to adipogenic induction. ADSCs retrieved from animals exposed to TBT *in utero* showed increased expression of PPARγ target genes such as the early adipogenic differentiation gene marker fatty acid-binding protein 4 and hypomethylation of the promoter/enhancer region of the fatty acid-binding protein 4 locus. Hence, TBT alters the stem cell compartment by sensitizing multipotent stromal stem cells to differentiate into adipocytes, an effect that could likely increase adipose mass over time. (***Molecular Endocrinology*** **24: 526–539, 2010)**

A single risk factor is rarely responsible for the development of most chronic diseases. The major factors driving obesity are most often ascribed to genetics (1) and behavioral factors such as smoking (2), excessive consumption of alcohol (3) and food (4), stress (5), and sedentary lifestyle (6). Infectious agents may also contribute to obesity and type 2 diabetes (7, 8). Childhood and adult obesity are among the cardiovascular risks that are considered to be programmed by early life experiences. Perhaps counter intuitively, babies subjected to either nutritional deprivation or to an environment overly rich in nutrients appear to be at risk for later development of obesity and diabetes (9). The retrospective cohort studies of David Barker and colleagues (10) during the late 1980s established the principle that the incidence of certain adult metabolic abnormalities may be linked to *in utero* development. This concept is often referred to as the "developmental origins of health and disease" (DoHAD) paradigm.

The biological mechanisms underlying the developmental origins of metabolic diseases remain poorly understood. Extensive human epidemiological studies and data from animal models indicate that maternal nutrition, and other environmental stimuli during critical periods of prenatal and postnatal mammalian development, influ-

ISSN Print 0888-8809 ISSN Online 1944-9917
Printed in U.S.A.

doi: 10.1210/me.2009-0261 Received July 2, 2009. Accepted December 30, 2009.
First Published Online February 16, 2010

Abbreviations: ADSCs, Adipose-derived stromal stem cells; ADIPOQ, adiponectin; ALP, alkaline phosphatase; α-MEM, α-MEM without nucleosides; BMSCs, bone marrow-derived stem cells; CMC, carboxymethyl cellulose; COL, collagen; DMSO, dimethylsulfoxide; DoHAD, Developmental Origins of Health And Disease; E16.5, embryonic d 16.5; Fabp4, fatty acid-binding protein 4 (aka aP2); LEP, leptin; MDII, isobutylmethylxanthine, dexamethasone, insulin, indomethacin adipogenic cocktail; MSC, multipotent stromal cell/mesenchymal stem cell; PPARγ, peroxisome proliferator-activated receptor γ; Pref-1, adipocyte differentiation-associated Protein; ROSI, rosiglitazone; RXR, retinoid X receptor; OPN, osteopontin; TBT, tributyltin; TTNPB, 4-(E-2-[5,6,7,8-tetrahydro-5,5,8,8-tetramethyl-2-naphthalenyl]-1-propenyl) benzoic acid.

ence developmental pathways and thereby induce permanent changes in metabolism and susceptibility to chronic disease (11–14). Emerging evidence suggests that alterations in epigenetic marking of the genome *in utero* can influence gene expression, and therefore, phenotype (15). Extensive covalent modifications to DNA and histone proteins occur from the earliest stages of mammalian development. Because these modifications influence lineage-specific patterns of gene expression, they represent a plausible mechanism through which environmental factors can perturb normal development or homeostasis. Altered mitochondrial function (13), increased DNA methylation, and histone deacetylation are the most studied epigenetic mechanisms shown to silence gene expression. DNA methylation controls the activity of mammalian promoter regions and might also be involved in the loss of stem cell pluripotency and in cellular specification (16). Interestingly, epigenetic modifications of peroxisome proliferator-activated receptors (PPARs) might be involved in the fetal adaptations to maternal diet and in the programming of subsequent metabolic abnormalities in later life (17). Recent evidence also supports an important role for environmental factors in obesity that could be programmed *in utero*. Among these is the exposure to endocrine-disrupting chemicals (18–20). As obesity and related metabolic syndrome disorders reach epidemic levels worldwide, the study of how environmental chemicals impact the etiology of obesity, particularly via maternal exposure, is timely and important.

The widespread use of organotin compounds, such as tributyltin (TBT), in agriculture and industry has led to the release of significant amounts of these compounds into the environment. Human exposure to non-point sources of organotins occurs through seafood dietary sources stemming from use of TBT as an antifouling agent on boat hulls and from organotin use as fungicides on food crops. Additional exposure comes from organotin use as fungicides on timber products, as well as from leaching of organotin-stabilized polyvinyl chloride from water pipes, food wrap, and other plastics (21, 22). TBT is best known as an endocrine disrupter that decreases aromatase activity, thereby increasing testosterone levels and causing imposex in female gastropod mollusks (23). TBT exposure can also transform females into males in some fish species (24, 25) but has not been reported to alter sex ratio in mammals (26).

The environmental obesogen model proposes that chemical exposure during critical stages in development can influence subsequent adipogenesis, lipid balance, and obesity (18, 20, 21). Obesogens can be functionally defined as chemicals that inappropriately alter lipid homeostasis and fat storage, metabolic setpoints, energy balance, or the regulation of appetite and satiety to promote fat accumulation and obesity (18, 19, 21). TBT is an obesogen because it induces adipogenesis in cell culture models and increases adipose mass *in vivo* in two vertebrate model organisms, frogs and mice (19). TBT is an agonistic ligand with nanomolar affinity for both the retinoid X receptors (RXRs) and peroxisome proliferator-activated receptor γ (PPARγ). TBT promotes adipogenesis in the murine 3T3-L1 preadipocyte model, and perturbs key regulators of adipogenesis and lipogenic pathways *in vivo* (19). Moreover, *in utero* exposure to TBT led to strikingly elevated lipid accumulation in adipose depots, liver, and testis of neonatal mice and resulted in increased epididymal adipose mass in adults (19). Thus, prenatal exposure to TBT causes changes that lead to fat accumulation in adults, despite access to normal diet and exercise. Because TBT is clearly an obesogen, it is important to define the mechanisms underlying the effects of prenatal exposure on adult physiology.

The onset of obesity involves extensive remodeling of adipose tissue at the cellular level and is dependent on the coordinated interplay between adipocyte hypertrophy (increase of cell size) and hyperplasia (increase of cell number). Until recently it was believed that the size of the adipocyte progenitor pool is established during development (27). In this view, initial pool size remains a dominant determining factor for adipogenesis, although recruitment of additional adipocyte progenitors, increased preadipocyte proliferation, and enhanced differentiation in adults may also be involved. In an as yet unknown manner, the fate of pluripotent stem cells is further restricted to multipotent mesenchymal stem cells, now called "multipotent stromal stem cells" (MSCs) during embryonic development of adipose tissue (27, 28). MSCs are plastic-adherent fibroblasts found in several tissues, including the bone marrow and fat, which have the ability to differentiate into multiple specialized cell types *in vitro* and *in vivo*. These include (but are not limited to) osteoblasts, chondrocytes, adipocytes, myocytes, and neurons (29). MSCs have emerged as a model to study adipogenesis because they exhibit gene expression profiles during differentiation comparable to that of other *in vitro* models, such as 3T3-L1 cells (30). The antidiabetic agent rosiglitazone (ROSI) is a highly specific agonist of PPARγ that is known to induce adipogenesis in a variety of cell culture models, including MSCs (31). It is believed that ROSI induces MSCs to differentiate into adipocytes through the modulation of PPARγ activity (although this has not been formally proven) and that PPARγ controls the lineage allocation of bone marrow MSCs between adipocytes and osteoblasts (32). Therefore, PPARγ ago-

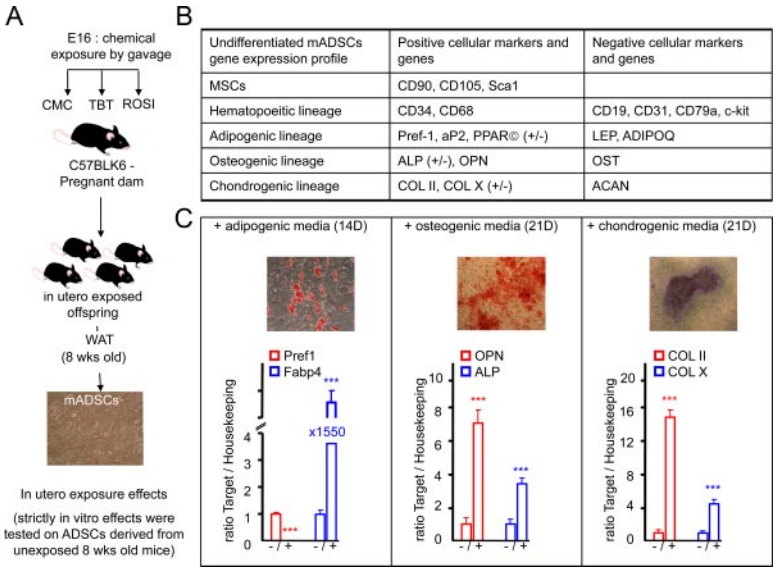

Undifferentiated mADSCs gene expression profile	Positive cellular markers and genes	Negative cellular markers and genes
MSCs	CD90, CD105, Sca1	
Hematopoeitic lineage	CD34, CD68	CD19, CD31, CD79a, c-kit
Adipogenic lineage	Pref-1, aP2, PPARγ (+/-)	LEP, ADIPOQ
Osteogenic lineage	ALP (+/-), OPN	OST
Chondrogenic lineage	COL II, COL X (+/-)	ACAN

FIG. 1. Experimental design and characterization of mADSCs. A, Study of the effect of prenatal TBT exposure. The effect of fetal and neonatal exposure to TBT was observed in C57BL/6J mice exposed to the chemical *in utero*. Pregnant females were dosed by gavage feeding with 0.1 mg/kg TBT, 1 mg/kg ROSI, or 0.5% CMC vehicle at E16.5. At 8 wk of age, mice were killed to isolate ADSCs from n = 5 pooled WAT. Subsequent treatment with nuclear receptor agonists is described in Figs. 2 and 5. B, Gene expression profile of mADSCs for multilineage progenitors and surface markers. The presence or absence of surface markers or transcripts specific to adipogenic, osteogenic chondrogenic lineages was detected by real-time RT-PCR in undifferentiated mADSCs, with the expression of each target gene normalized to β-actin. A gene was considered not expressed in the cell preparation if its mean Ct value exceeded 38. The symbol (+/−) was assigned to genes the expression of which was low (mean Ct value exceeding 32), but consistently detectable. C, Multilineage assays. ADSCs were differentiated into adipose (A), bone (B), and cartilage (C) throughout the experiments (up to passage 6). The expression level of specific lineage markers was assayed by real-time PCR as previously described. Adipogenic (LEP, ADIPQ), osteogenic (OST), and chondrogenic (ACAN) markers that were not significantly expressed in undifferentiated cells, were detectable in induced mADSCs. Data were expressed as average fold change in expression ± SEM in differentiated relative to undifferentiated ADSCs. *Asterisks* represent significant differences (***, $P < 0.001$). ACAN, Aggrecan; OST, osteocalcin.

nists such as TBT and similar organotins could profoundly impact the stem cell compartment.

Prenatal and early postnatal events, such as maternal nutrition, drug, and chemical exposure, are received, remembered, and then manifested in health consequences later in life. Based on the observed effects of TBT on adipogenesis, we hypothesized that organotin exposure during prenatal adipose tissue development changes the potency of the MSC progenitor pool to favor adipocytes. In support of this theory, we show here that TBT sensitizes multipotent stem cells derived from both human (h) adipose-derived stem cells (ADSCs) and mouse (m) ADSCs white adipose tissue to undergo adipogenesis *in vitro*. Using a mouse model we found that prenatal TBT exposure modifies the stem cell compartment to favor the production of adipocytes. TBT exposure is associated with changes in DNA methylation in the MSC population, and prenatal TBT exposure increased expression of adipocyte-specific genes. Thus, TBT exposure during early life alters the balance of progenitor types in the stem cell compartment to favor the production of adipocytes. Our results provide a potential explanation for the obesogenic properties of TBT and illustrate more generally how prenatal exposure to xenobiotic compounds could affect adipogenesis and obesity.

Results

Characterization of the stem cell models

The effect of TBT exposure on adipogenic capacities was first assayed *in vitro* using human and mouse MSCs retrieved from white adipose tissue (WAT) not previously exposed to the chemical. The use of a mouse model also allowed the investigation of the effect of TBT exposure during fetal and early life, *ex vivo*, by harvesting the same cells in young adults after they were exposed to TBT *in utero*, as summarized in Fig. 1A.

The gene expression profiles of the adherent cell population we isolated from C57BL6/J WAT were consistent with expectations for an MSC-enriched population (Fig. 1B). mADSCs expressed high levels of MSC surface markers (CD90, CD105, and Sca1), whereas hematopoietic surface markers (CD19, CD31, CD79a, c-kit) were virtually absent. Exceptions were CD34, which is found in our mADSC preparation, as others observed in mouse stem cell models (33), and CD68, a macrophage marker that was also expressed. Markers for early differentiation into adipocytes [PPARγ2 and fatty acid-binding protein 4 (Fabp4) also known as aP2], osteoblasts [alkaline phosphatase (ALP) and osteopontin (OPN)] and chondrocytes [type II collagen (COL II); and type X collagen (COL X)] were low but detectable. Markers for late stages of adipogenesis [leptin (LEP); and adiponectin (ADIPOQ)], osteogenesis osteocalcin, and chondrogenesis (aggrecan) were virtually absent.

To verify that the mADSCs maintained their multipotent nature, cells were differentiated into cartilage, adipose, and bone regularly throughout the experiments. When exposed for 14–21 d to the appropriate induction media, all cell types showed the ability to differentiate into adipocytes, osteocytes, or chondrocytes as indicated by intracellular lipid accumulation (Oil Red O), extracellular matrix calcification (Alizarin Red), or proteo- and glucosamino-glycan staining (toluidine blue O), respectively (Fig. 1C). The capacity of the MSCs to differentiate

into various lineages was also assessed by analyzing mRNA for a panel of molecular markers. During the early stages of adipocyte development (2 d), the PPARγ target gene Fabp4 is induced in preadipocytes (34, 35), whereas adipocyte differentiation-associated protein (Pref-1), an inhibitor of adipocyte differentiation, is decreased (36) (Fig. 1C). Late events (14 d) include the synthesis of adipocyte-secreted products such as LEP and ADIPOQ (37) that we were able to detect at high levels in differentiated cells (data not shown). Differentiation into osteoblasts on the other hand, involved an early increase in ALP gene expression and an intermediate increase in OPN (Fig. 1C), followed by a late increase in OSC gene expression (data not shown) (38, 39). Differentiation along the chondrogenic lineage is revealed by early increases in collagen molecules (COL II and COL X) (Fig. 1C) and late aggrecan expression (data not shown) (40). Therefore, we conclude that the cell populations employed in the following experiments are representative of the multipotent stem cell types found in mouse adipose tissue.

hADSCs were characterized by the provider (Invitrogen, Carlsbad, CA) using flow cytometry. Passage 1 hADSCs were positive for CD29, CD44, CD73, CD90, CD105, and CD166 (>95%) and negative for CD14, CD31, CD55, and Lin1 (<2%). hADSCs have at least bipotential differentiation capacities and as with mADSCs, we verified that these cells retained their ability to differentiation into osteoblasts throughout the experiments (data not shown).

In vitro exposure to TBT enhances differentiation of human and mouse MSCs into adipocytes

MSCs from male or female mice had a similar capacity to form adipocytes (data not shown). Consequently, all data presented were obtained using female mice. When adipogenic differentiation was induced in mADSCs by treatment with standard adipocyte induction cocktail (isobutylmethylxanthine, dexamethasone, insulin, indomethacin; MDII) and dimethylsulfoxide (DMSO) vehicle, cells with lipid droplets covered approximately 20% of the dish surface (Fig. 2A). About 30% of the cells contained lipid droplets (although the number and size of droplets were variable). Lipid accumulation was increased in the cells exposed to adipogenesis cocktail supplemented with 50 nM TBT or 50 nM of the PPARγ agonist ROSI, and the surface covered with lipid reached 55% (65–75% of the total number of cells contain lipids) (Fig. 2A). At 5 nM, TBT failed to increase lipid accumulation or the number of cells containing lipids, showing the dose dependency of the effect. The RXR-selective agonist AGN195203 (AGN) at 50 nM did not significantly increase lipid accumulation or the number of cells with lipids, suggesting a less pronounced effect on adipogenesis by RXR activation, compared with the PPARγ activation by ROSI. As expected, the retinoic acid receptor activator, 4-(E-2-[5,6,7,8-tetrahydro-5,5,8,8-tetramethyl-2-naphthalenyl]-1-propenyl) benzoic acid (TTNPB), which is known to inhibit adipogenesis in 3T3-L1 cells (19), did not increase adipogenic capacity (Fig. 2A) and was used as a negative control in all experiments. Both TBT and ROSI at 50 nM were able to induce a modest amount of adipocyte differentiation (~20%), even in the absence of the adipogenic induction cocktail (data not shown), consistent with our observations in 3T3-L1 cells (19). A proliferation assay was performed to determine whether the cells were proliferating or instead terminally differentiating. The results showed that cells treated with MDII, which is known to induce differentiation, proliferated less (Fig. 2B). Both ROSI and TBT alone reduced proliferation in a dose-dependant manner, suggesting that PPARγ activation by these chemicals inhibits proliferation and favors adipogenic differ-

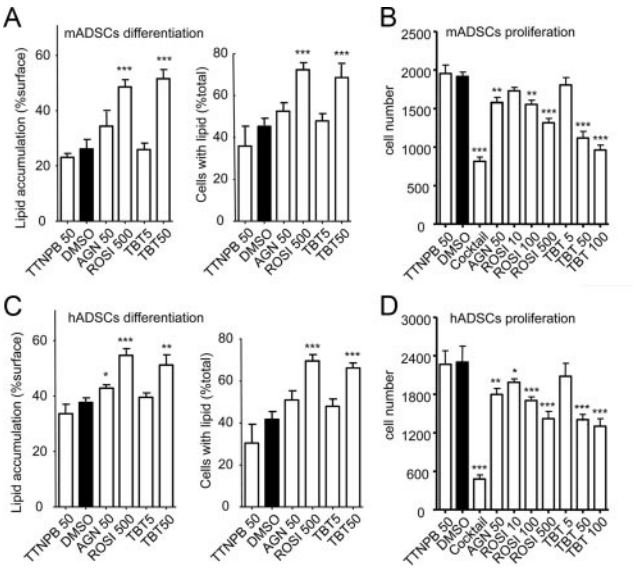

FIG. 2. *In vitro* effect of TBT exposure on ADSCs adipogenic and proliferative capacities. A, Adipogenesis was induced in mADSCs by the addition of an adipogenic cocktail for 14 d in the absence (DMSO) or presence of nuclear receptor agonists 50 nM TTNPB (RAR, negative control), 50 nM AGN (RXR), 500 nM ROSI (PPARγ), or two doses of TBT (5 and 50 nM) (n = 3 wells per treatment). Undifferentiated cells were kept in basic MSCs expansion media, able to prevent differentiation, as a negative control (untreated cells). Lipid accumulation was stained by Oil Red O and quantified with Image J software. The number of cells with lipid droplets was also visually counted. B, Proliferative capacities of mADSCs were assayed by CyQuant cell counting of culture in regular expansion media, with 400 cells as a starting quantity. Media was supplemented with DMSO, adipogenic cocktail, 50 nM TTNPB, 50 nM AGN, 10, 100, or 500 nM ROSI, or 5, 50, or 100 nM TBT (n = 3 wells per treatment and time point, n = 3 pictures per well). C, Adipogenic capacities of hADSCs were performed as described for hADSCs. Mouse cells were isolated as described in Fig. 1. All data were expressed as average fold change in n = 9 replicates ± SEM (n = 3 wells per treatment in triplicates) relative to vehicle (DMSO) controls. *Asterisks* show significant differences (*, $P < 0.05$; **, $P < 0.01$; ***, $P < 0.001$). D, Proliferative capacities of hADSCs harvested from mice not prenatally exposed to RXR and/or PPARγ ligands.

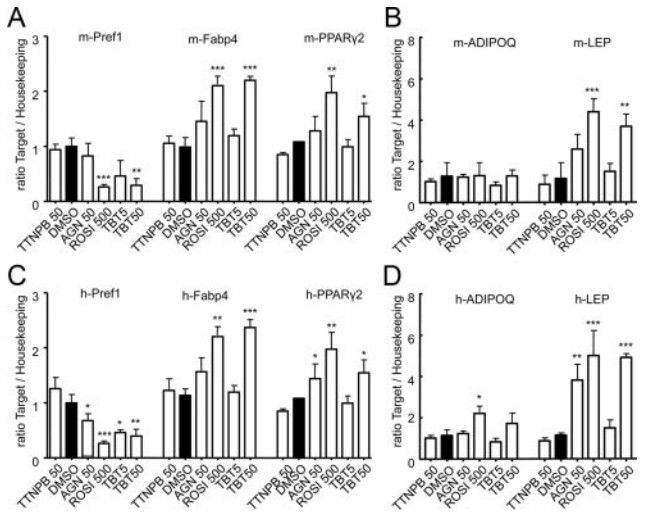

FIG. 3. *In vitro* effect of TBT exposure on adipogenic markers in differentiated ADSCs. Gene expression profile of adipogenesis-induced hADSCs (panels A and B) and mADSCs (panels C and D) was assayed by real-time RT-PCR (1. Early adipogenesis markers: Pref-1, Fapb4, and PPARγ2 (panels A and C); 2. Late adipogenesis markers: ADIPOQ and LEP, panels B and D). Expression was normalized to β-actin and expressed as average fold change in expression ± SEM (n = 3 wells per treatment in triplicates) relative to vehicle (DMSO) controls.

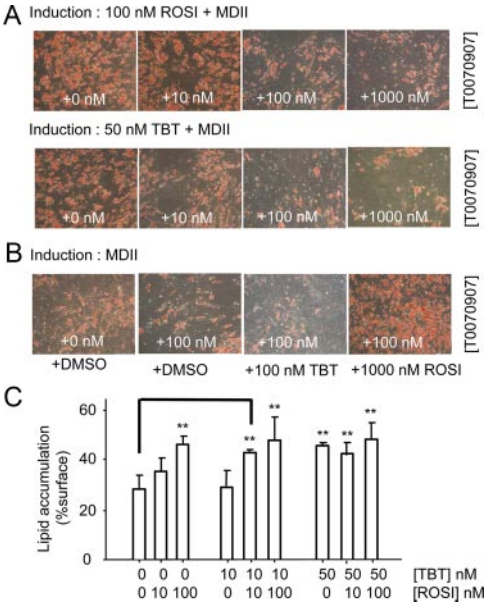

FIG. 4. Effect of the PPARγ2 agonist ROSI, and the PPARγ2 antagonist T0070907 on the TBT-induced increase of the adipogenic abilities of mADSCs *in vitro*. Mouse cells were isolated as described in Fig. 1. All pictures are representative of n = 9 replicates ± SEM (n = 3 wells per treatment in triplicate) relative to vehicle (DMSO) controls. *Asterisks* show significant differences (*, $P < 0.05$; **, $P < 0.01$; ***, $P < 0.001$). Lipid accumulation was stained by Oil Red O and quantified with Image J software. A, Adipogenesis was induced in mADSCs by the addition of an adipogenic cocktail for 14 d with 100 nM ROSI (*upper row*) or 50 nM TBT (*lower row*) in the presence of DMSO, 10, 100, or 1000 nM T0070907 (PPARγ antagonist). B, Adipogenesis was induced in mADSCs by the addition of an adipogenic cocktail with 0 or 100 nM T0070907 for 14 d in the presence of DMSO, 100 nM TBT, or 1000 nM ROSI. C, Adipogenesis was induced in mADSCs by the addition of an adipogenic cocktail for 14 d with three doses of ROSI (0, 10, and 100 nM) in combination with three doses of TBT (0, 10, 50 nM). Data were expressed as average fold change in n = 9 replicates ± SEM (n = 3 wells per treatment in triplicate) relative to vehicle (DMSO) controls.

entiation of the mADSCs. All assays were repeated in the human model using MSCs derived from WAT. The results observed in hADSCs on adipogenic capacities (Fig. 2C) and proliferative capacities (Fig. 2D) were virtually the same.

After exposure to the standard adipogenesis induction cocktail MDII, expression of all adipogenesis markers changed dramatically compared with unexposed cells (Fig. 1, B and C). Measurement of mRNA levels by quantitative real time RT-PCR (QPCR) at the end of the 14-day induction/differentiation period revealed a gene expression profile consistent with enhanced adipogenesis in the mADSCs exposed to TBT *in vitro* (Fig. 3, A and B). The early adipogenesis markers Fapb4 and PPARγ (~2-fold), and the late marker LEP (~4-fold) were significantly increased, whereas the adipogenesis inhibitor Pref-1 was decreased (~2.5-fold) when MDII was supplemented with 50 nM ROSI or TBT (Fig. 3, A and B). As previously observed, hADSCs responded to TBT and ROSI exposure *in vitro* (41); however, we also found that hADSCs were more affected by AGN than were mADSCs. In contrast to mADSCs, hADSCs showed significant inhibition of Pref-1 (Fig. 3C) and activation of LEP (Fig. 3D) mRNA levels when exposed to AGN. This suggests that RXR homodimers play a larger role in human adipocyte differentiation than in mouse, or that the human RXR:PPARγ heterodimer is more sensitive to AGN than is the corresponding mouse heterodimer. At 5 nM, TBT significantly inhibited Pref-1 expression in hADSCs, suggesting that even this low dose could push the cells toward an adipocyte fate and might produce mature adipocytes if the experiment had been maintained longer. No other difference was noted between the mouse and human models.

Overall, treatment with TBT or ROSI favored entry into the adipogenic pathway in both human and mouse ADSC models and induced a 25% increase in lipid accumulation in the number of cells containing lipid, compared with the MDII/DMSO control baseline. These cells also exhibited a gene expression profile consistent with increased adipogenesis. Thus, *in vitro* exposure to TBT inhibits proliferation and induces adipogenic differentiation in these multipotent stem cells.

In the presence of 100 nM ROSI or 50 nM TBT, adipogenic differentiation of mADSCs was dramatically reduced by the addition of the potent PPARγ antagonist T0070907 at concentrations as low as 100 nM. This suggests that PPARγ activation is required for the TBT-induced increase in adipogenic capacities (Fig. 4A). After

exposure to the standard adipogenesis induction cocktail MDII alone, T0070907 was also able to limit lipid accumulation in mADSCs (Fig. 4B). Under these conditions, the addition of 1000 nM ROSI restored the increase in lipid accumulation, whereas 100 nM TBT did not. This is not unexpected because doses of TBT of 200 nM or higher are toxic and the K_d of TBT for PPARγ (20 nM) is similar to that of T0070907 (40 nM). Thus, it is possible achieve a significant enough molar excess of ROSI to antagonist (10-fold) to reverse the inhibitory effect; however, it is not possible to achieve this for TBT due to toxicity. Similar observations were obtained with hADSCs (Supplemental Fig. 1 published on The Endocrine Society's Journals Online web site at http://mend.endojournals.org). We next asked whether TBT and ROSI could act synergistically to induce lipid accumulation in mADSCs (Fig. 4C). The addition of 10 nM TBT or 10 nM ROSI alone did not cause an increase in lipid accumulation; adding both chemicals at this concentration significantly induced adipogenesis in ADSCs (Fig. 4C). Taken together, the synergistic induction of adipogenesis by TBT and ROSI, and the inhibition of adipogenesis by the PPARγ antagonist, indicates that induction of adipogenic differentiation by TBT in ADSCs is PPARγ mediated.

Prenatal exposure to TBT promotes adipogenic and osteogenic differentiation in mouse ASDCs

To ascertain the lowest dose able to induce an acute (24 h) response of hepatic PPARγ target genes for use in subsequent *in vivo* experiments, adult females were dosed by gavage feeding with TBT followed by analysis of hepatic gene expression (Supplemental Fig. 2). The results indicate that 0.1 mg/kg was the lowest TBT dose that reliably induced the expression of fatty acid synthase, fatty acid transport protein, acetyl-CoA-carboxylase, and sterol response element-binding protein 1c. Similar results were obtained when TBT was administered by ip injection and when males were dosed (Supplemental Fig. 3). Therefore, 0.1 mg/kg TBT was adopted for all *in vivo* experiments.

To observe the effects of TBT exposure on the offspring, pregnant females were dosed by gavage feeding with TBT at 0.1 mg/kg, ROSI at 1 mg/kg, or carboxylmethyl cellulose (CMC) vehicle at 0.5% at embryonic d 16.5 (E16.5). Stromal cells were isolated from WAT of 8-wk-old mice that had been exposed *in utero* to PPARγ agonists or CMC control. Treatment of mADSCs with adipogenesis cocktail revealed that cells derived from prenatally TBT- or ROSI-exposed animals exhibited an increase in their adipogenic differentiation capacities. Prenatal TBT or ROSI treatment led to a 2-fold increase in the total lipid accumulation (from 20% to 40%) compared with CMC-exposed controls without the addition of ligands to the assay (Fig. 5A). Consistent with the *in vitro* assays shown above (Figs. 2 and 3) an additional *in vitro* exposure of these cells to 50 nM TBT or 500 nM ROSI further increased lipid accumulation above DMSO control baselines. Addition of TBT to cells derived from prenatally ROSI or TBT-treated mice caused a 1.8-fold increase in lipid accumulation and led to very high levels of lipids (~70% of total area) of CMC-exposed mice, compared with the DMSO control (Fig. 5A). As would be predicted by these observations, we found that expression of Fapb4 (Fig. 5B) and LEP (Fig. 5C) was increased more than 2-fold in TBT- and ROSI-exposed mice compared with CMC. Additional exposure to TBT or ROSI *in vitro* caused a significant further increase in Fapb4 mRNA levels, whereas only additional TBT exposure elicited a significant additional increase in LEP mRNA levels.

When bone differentiation was induced by the osteogenic cocktail in mADSCs derived from CMC-treated animals, 80% of the extracellular matrix surface was calcified (Fig. 6A). Prenatal ROSI or TBT treatment decreased the osteogenic capacity of these cells 2-fold and 2.8-fold, respectively. In accord with these results, expression of mRNA encoding the bone marker OPN was reduced by 2-fold in ROSI- or TBT-exposed mice (Fig. 6B). Supplementation with TBT *in vitro* caused a >3.5-fold decrease in bone differentiation and OPN gene expression in CMC-exposed animals, but had little to no additional effect on osteogenic and adipogenic capacities of ROSI- and TBT-exposed mice (Fig. 6, A and B). In contrast, when ADSCs treated with osteogenic cocktail were supplemented with TBT *in vitro*, spontaneous adipogenic differentiation was observed in prenatally ROSI- and TBT-exposed mice, with lipid accumulation covering 5 and 25% of the mADSCs surface, respectively (Fig. 6A). Expression of the adipogenesis marker aP2 was also dramatically increased in these groups, with a 600- and 750-fold increase of aP2 mRNA levels in ROSI- and TBT-exposed mice, respectively. This suggests that TBT exposure facilitates adipogenic differentiation to the detriment of osteogenic differentiation in mADSCs.

Prenatal TBT exposure modifies the molecular signature of the stem cell compartment to favor adipogenesis

The data presented above suggest that prenatal exposure to the PPARγ activators TBT or ROSI biased the stem cell compartment toward the adipocyte lineage. To test this hypothesis, we analyzed expression of a panel of molecular markers in undifferentiated ADSCs derived from prenatally treated animals. Alterations in gene expression should reflect TBT-induced changes in the na-

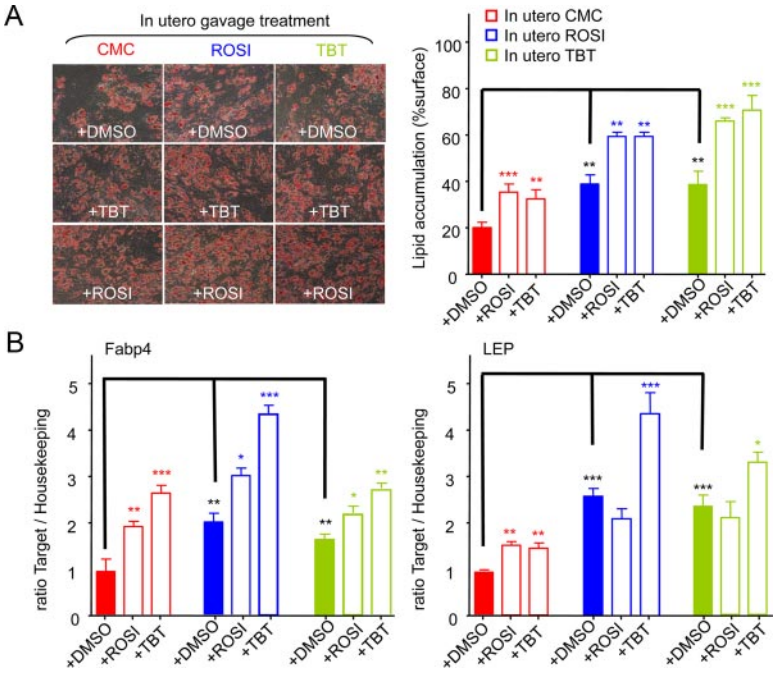

FIG. 5. Effect of TBT prenatal exposure on adipogenic capacities of mADSCs. TBT and ROSI exposure *in utero* was performed as described in Fig. 1. mADSCs harvested from exposed animals was additionally treated *in vitro* with 50 nM TBT, 500 nM ROSI [PPARγ agonist]), or a DMSO vehicle control, in the presence of an adipogenic induction cocktail (n = 3 wells per treatment in triplicates) for 14 d. Undifferentiated cells were kept in basic MSCs expansion media, able to prevent differentiation, as a negative control (untreated cells). A, Lipid accumulation was stained by Oil Red O and quantified by Image J software. Mice *in utero* treatments are presented from *left to right* (CMC, TBT, and ROSI). Additional *in vitro* TBT and ROSI treatments of ADSCs are presented from the *bottom* up. B, Gene expression profile of adipogenesis-induced mADSCs was assayed by real-time RT-PCR as previously described (early adipogenesis markers: Pref-1 and Fapb4; late adipogenesis marker: LEP), using cells treated with cocktail only (+DMSO vehicle control) as a reference group. *Asterisks* show significant effects of *in utero* (*black bars*) and *in vitro* treatments.

ture of the MSC population. We found that TBT exposure caused an increase in Fapb4 and PPARγ mRNA (Figs. 6B and 7A). Tchoukalova *et al.* (42) defined a precursor cell committed to the adipogenic lineage as an Fapb4-positive cell (preadipocyte). Macrophages also express Fapb4, together with a surface marker not found on preadipocytes (CD68). Because expression of CD68 is unchanged after TBT exposure, this suggests the increase in Fapb4 expression is not due to an increase in the number of macrophages. Moreover, because both the amount of lipid accumulation and the number of cells containing lipid is increased in ADSCs derived from *in utero* TBT-exposed mice (Fig. 5), it is likely that the number of cells expressing Fapb4 is increased. This was confirmed by flow cytometry. We found that before any induction of differentiation, the number of preadipocytes was increased by approximately 6% in the undifferentiated cells derived from animals exposed to TBT and ROSI, respectively, compared with the CMC control (Fig. 7B). These data support a model wherein prenatal TBT exposure enriched the MSC population with cells committed to the adipocyte lineage.

Prenatal TBT exposure causes reduced DNA methylation in the stem cell compartment that favors formation of adipocytes

Changes in potency of stem cells can be associated with altered methylation of DNA and modification (*e.g.* methylation, acetylation, sumoylation) of chromatin-associated histones. To determine whether such changes were found in ADSCs from TBT-exposed animals, we first examined the methylation status of the promoter/enhancer regions of Fabp4 and PPARγ2 using methylation-sensitive restriction enzymes. Three potential cytosine methylation sites exist in Fabp4 that could alter restriction digestion by restriction enzyme *Aci*I, whereas one potential methylation site exists in PPARγ2 that could alter digestion by *Acl*I (Fig. 8A). DNA was prepared from ADSCs derived from prenatally TBT- or CMC-treated animals, digested with *Aci*I or *Acl*I, and subjected to real-time PCR analysis. Comparison of the Ct values from the three potentially methylated regions (aP-Met1, aP-Met2, and aP-Met3) with those from a region not expected to be cut by *Aci*I (uncut in Fig. 8A), showed that *Aci*I digestion of template was 2-fold increased when the ADSCs were derived from *in utero* TBT-exposed animals, compared with the CMC-exposed control (Fig. 8B). This suggests that one mechanism underlying the overexpression of Fapb4 in mADSCs derived from TBT-exposed animals involves an undermethylation of its promoter/enhancer region. Digestion of the PPARγ2 promoter/enhancer region by *Acl*I was unaffected by prenatal TBT exposure (Fig. 8B), which is consistent with the observation that expression of PPARγ2 mRNA was not increased by prenatal TBT exposure (Fig. 7A).

Discussion

The results presented above demonstrate that *in utero* exposure to TBT enhances the capacity of a population of stem cells in adult mouse WAT to form adipocytes. Most mechanistic studies to date have employed the murine 3T3-L1 cell model, a population of fibroblasts already committed to the adipogenic pathway (43). Due to their ability to differentiate into many different cell types, multipotent stem cells have recently become a popular model

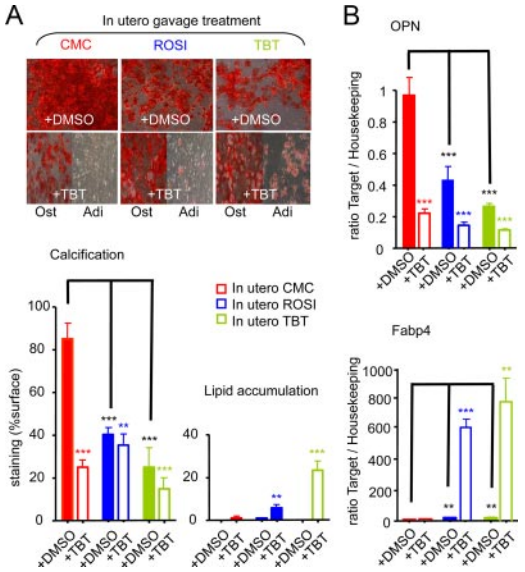

FIG. 6. Effect of TBT prenatal exposure on osteogenic capacities of mADSCs. TBT and ROSI exposure *in utero* was performed as described in Fig. 1. mADSCs harvested from exposed animals were additionally treated *in vitro* with 50 nM TBT or a DMSO vehicle control, in the presence of an osteogenic induction cocktail (n = 3 wells per treatment in triplicate) for 21 d. Undifferentiated cells were kept in basic MSC expansion media (which did not allow differentiation), as a negative control (untreated cells). A, Calcium accumulation was stained by Alizarin Red S and quantified by Image J software. Mice *in utero* treatments are presented from *left to right* (CMC, TBT, and ROSI). Additional *in vitro* TBT treatment of ADSCs are presented on *lower rows*, with calcium accumulation (Ost, *left panel*) and lipid accumulation (Adi, *right panel*), performed as previously described. B, Gene expression profile of osteogenesis-induced mADSCs was assayed by real-time RT-PCR as previously described (adipogenesis markers: Fapb4; osteogenesis marker: OPN), using cells treated with cocktail only (+DMSO vehicle control) as a reference group. *Asterisks* show significant effects of *in utero* (*black bars*) and *in vitro* treatments. Ost, Osteocalcin; Adi, adipocyte.

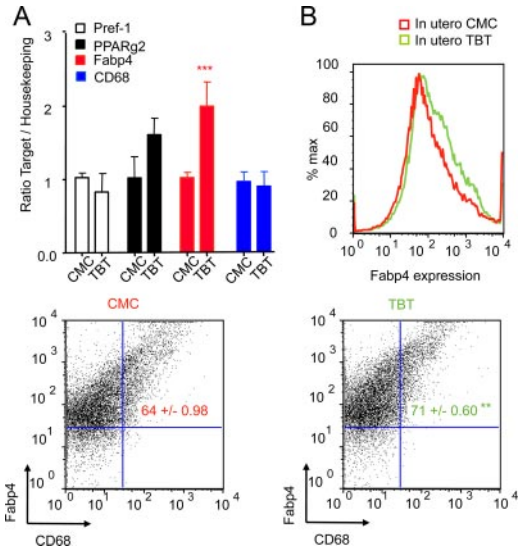

FIG. 7. Effect of prenatal TBT exposure on the gene expression profile of undifferentiated mADSCs. TBT exposure *in utero* was performed as described in Fig. 1. A, Undifferentiated mADSCs were cultured, and gene expression levels of marcrophage surface and adipogenic markers were assayed by real-time RT-PCR with the expression of each target gene normalized to β-actin. Data were expressed as average fold change in expression ± SEM (n = 3 per treatment in triplicates) relative to CMC controls. B, Flow cytometry. Undifferentiated mADSCs were cultured, and the number of CD68- and Fabp4-postive cells were counted. The *upper panel* is a frequency histogram displaying the Fabp4 relative fluorescence plotted against the total number or events (maximum number of cells) from untreated mADSCs harvested from animals *in utero* exposed to CMC (*red*) or TBT (*green*). The *two lower panels* are the density plots for the same population of cells, with the x- and y-axis representing the CD68 and Fabp4 fluorescence, respectively, and the cell count height on a density gradient. Particle counts are shown by dot density. The Fabp4-positive but CD68-negative cells, thought to be preadipocytes, appear in the *boxed upper left quadrant* of the histogram.

with which to study differentiation processes, including adipogenesis. We chose the MSC model because it is more relevant to the fate of adipose tissue, *in vivo*. Adipose tissue originates from the differentiation of pluripotent stem cells of mesodermal origin into more restricted multipotent stem cells, and then to adipocyte progenitors during embryonic and early neonatal developmental (27). The molecular signatures of hADSCs, as well as the mADSCs isolated for this study, were consistent with an MSC-enriched population (44). Moreover, we showed that ADSCs retained their multipotency throughout the course of the experiments. Adipogenic capacities were assayed by the appearance of lipid droplets but also by the modification of the transcriptional signature of the cells undergoing differentiation. We observed that in both human and mouse models, increased lipid accumulation in ADSCs was always concomitant with an increase in the expression of mRNAs encoding the early adipogenic markers PPARγ and Fapb4, the late marker LEP, and a decrease in adipogenesis inhibitor Pref-1.

Carfi' *et al.* (45) showed a significant increase in the number of adipocytes, and a decrease in the number of hematopoietic markers, in TBT-treated human bone marrow-derived MSCs (BMSCs). Our results using mouse and human stromal stem cell populations derived from WAT *in vitro* support this observation (Fig. 2). It is still unclear whether hyperplastic growth *in vivo* is due to differentiation of resident MSCs within the adipose tissues or from BMSCs outside of the adipose tissues through mobilization, circulation, and recruitment. Crossno *et al.* (46) offered the first direct evidence that nonresident progenitor cells contribute to the adipocyte population of adipose tissues. Their conclusions were questioned by similar studies of Koh *et al.* (47). These authors proposed that circulating BMSCs failed to differentiate in adipose tissues and attributed Crossno's observations to inadequate discrimination of adipocytes from neighboring macrophages. Our study does not address this controversy but extends these studies by showing that TBT alters the fate of resident MSCs in WAT by diverting them toward an adipocyte lineage.

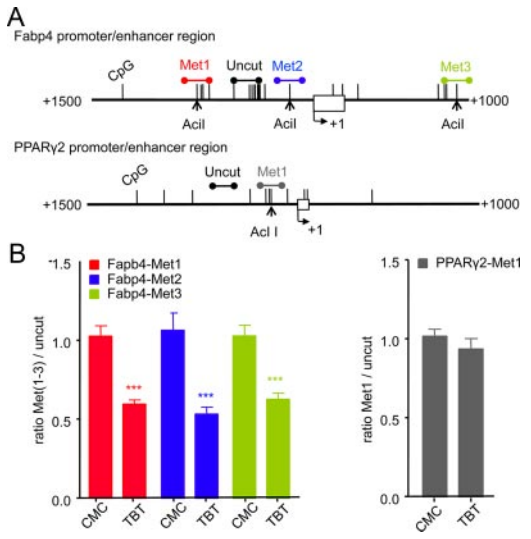

FIG. 8. Effect of prenatal TBT exposure on the methylation status of Fapb4 promoter/enhancer region. A, Fapb4 and PPARγ2 promoter/enhancer regions. Schematic representation of the CpG islands, which spans −1500 to +100 with respect to the transcription initiation site (*right angle arrow* at +1) and restriction map (*arrows*). The *closed box* represents the location of Exon1, and the *vertical bars* represent the location of CpG sites. *Horizontal bars* represent the fragments (Met1, Met2, and Met3) spanning the restriction sites and the uncut control amplified by real-time RT-PCR. B, Occurrence of methylation in Fapb4 and PPARγ2 promoter/enhancer regions. Genomic DNA extracted from undifferentiated mADSCs harvested from TBT- or CMC-exposed mice was digested by the methylation-sensitive enzyme *AciI*. Uncut fragments corresponding to potentially methylated were detected by real-time RT-PCR with the expression of each target normalized to a region without restriction sites (uncut). Data are presented as previously described.

Significantly, we provide the first evidence that TBT predisposes MSCs to become adipocytes in mice exposed to TBT *in utero*. By favoring the entry of a significant part of the stem cell compartment into an adipogenic lineage, early TBT exposure could lead to the observed increase in adipose depot size in TBT-exposed animals. In this study, pregnant dams were given approximately 2.5 μg of TBT in a single dose by gavage feeding (0.1 mg/kg), which was found to acutely activate PPARγ target genes. TBT is routinely measured in wildlife and human blood and tissue samples in the range of 3–100 nM (48–50). In random human serum samples, TBT reached an average concentration (~27 nM) that is sufficient to activate high-affinity receptors such as RXR and PPARγ (for which the EC_{50} is ~20 nM) (19). Daily intakes of TBT oxide determined in Japan fluctuated between 1–7 μg/d (51). Therefore, the induction of adipogenic capacities we observed *in vitro* and *ex vivo* occurred at concentrations comparable to those encountered in humans, *in vivo*. Although it is important to note that specific aspects of metabolism and pharmacogenetics can differ significantly between mice and humans, we are unaware of any species-specific differences in activation of PPARγ by ligands. By extrapolation, our findings suggest that a significant fraction of the general population could be exposed to this compound at obesogenic concentrations.

How could TBT affect the differentiation of stem cells into adipocytes? Differentiation from a stem cell to a mature adipocyte involves several events (28, 52). The first phase, determination, corresponds to the commitment of a multipotent stem cell to the adipocyte lineage. These preadipocytes then undergo growth arrest and mitotic clonal expansion. During terminal differentiation, preadipocytes acquire the characteristics of mature adipocytes. The conversion of nonadipogenic fibroblasts into adipocytes in response to the ectopic expression of PPARγ requires exposure of the cells to an exogenous ligand, whereas differentiation of preadipocytes occurs without the addition of such a ligand (although there may be an as yet unidentified endogenous ligand) (53). However, the recent findings of Walkey and Spiegelman's (54) suggest that the binding and activation of PPARγ by agonist ligands may not always be required for adipocyte differentiation under physiological conditions. We showed that TBT has the ability to reduce proliferation of ADSCs, and to cause ADSC differentiation into adipocytes in culture. TBT leads to an increase in the number of ADSCs predisposed toward an adipocyte lineage at the expense of the osteogenic lineage *in vivo*, in prenatally exposed animals. The reciprocal relationship between adipocyte and osteocyte commitment and differentiation is well documented and is thought to involve a shift in the flow of mesenchymal precursor cells from osteoblastic to adipogenic lineages, an effect mediated by PPARγ (32). Our study confirms that such a shift between the two lineages occurs and that, as a PPARγ agonist, TBT is able to counteract osteogenesis and induce a preferential differentiation into adipocytes in both human and mouse ADSCs. The induction of adipogenic capacity by TBT in MSCs is likely to be mediated by activation of PPARγ because similar results were obtained when the cells or animals were exposed to the strong PPARγ activator ROSI, and because TBT and ROSI have synergic effects on the adipocyte differentiation in cultured ADSCs. More importantly, the effects of both ROSI and TBT are blocked by the addition of a PPARγ antagonist. The stronger activity of TBT is explainable by its action as a ligand for both RXR and PPARγ, which could cause additive or synergic effects (55). This interpretation is supported by the observation that the RXR ligand AGN, which can activate the RXR half of the permissive RXR-PPARγ heterodimer, can also lead to similar adipogenic effects (albeit more weakly).

Our data demonstrate that the ADSC compartment contains more cells the differentiation of which into adipocytes is facilitated by prenatal TBT or ROSI exposure. It is well

known that adipogenic and osteogenic progenitor cells are closely related (56). We cannot currently distinguish whether the larger population of adipogenic cells found in mADSCs from TBT- or ROSI-treated animals correspond to lineage-restricted preadipocytes (monopotential progenitors) or whether they are multipotential progenitors that retain plasticity or transdifferentiation capacity similar to mADSCs in untreated animals (56–58). Thus, the increased number of adipocyte that can be produced from ADSCs derived from prenatally TBT- or ROSI-exposed animals may reflect 1) more already committed adipocyte precursors, 2) changes in the balance in commitment choices of MSCs between osteoprogenitors and adipocyte progenitors, or 3) conversion of cells that would have become osteocyte progenitors into adipocyte progenitors. Post *et al.* (59) recently demonstrated the presence of independent preosteoblastic and preadipocytic cell populations in mouse BMSCs. This suggests that the MSC compartment could contain subpopulations of cells that are already committed to adipogenic, osteogenic, or other differentiation pathways. TBT exposure *in vitro* caused a dramatic decrease in osteogenic capacity together with a concomitant increase in spontaneous adipogenic differentiation in the stromal progenitor compartment (Fig. 5A). ADSCs exhibit a preadipocyte molecular signature with an increase in PPARγ and Fapb4 mRNA levels (Fig. 5B). Tchoukalova *et al.* (42) recently defined a preadipocyte as an Fapb4-positive cell, and we showed that TBT exposure caused a 2-fold increase in Fapb4 mRNA levels (Figs. 3 and 5). Using flow cytometry, we found that before any differentiation was induced, there was a significant increase in the number of cells expressing Fabp4 after prenatal TBT exposure (Fig. 7). This suggests that TBT exposure increased the number of preadipocytes in the stem cell compartment and/or committed at least a part of the ADSCs to an adipogenic lineage.

The rate at which obesity has increased suggests that environmental and behavioral influences, more than genetic changes, have fueled the epidemic. Epidemiological and experimental studies have recently highlighted the relationship between the periconceptual, fetal, and early infant phases of life and the subsequent development of adult adiposity (60). The DOHaD model proposes that the fetus adapts to adverse environmental cues *in utero* via epigenetic adjustments in gene methylation. Of particular interest is the Wingless protein pathway, which is thought to maintain preadipocytes in an undifferentiated state and to regulate cell fate by controlling PPARγ gene expression (61). Takada *et al.* (62) recently showed that the noncanonical Wingless protein pathway suppressed PPARγ function through chromatin inactivation, thus diverting MSCs toward an osteoblastic cell lineage. Thus, it is plausible that epigenetic modifications favoring expression of PPARγ target genes might be involved in the lineage shift we observed in the MSC compartment of animals prenatally exposed to TBT. We investigated the methylation status of the preadipocyte marker Fapb4 in undifferentiated mADSCs and confirmed that at least some sites of the promoter/enhancer region of the gene were hypomethylated in ADSCs derived from *in utero* TBT-exposed animals compared with controls (Fig. 8). Importantly, such changes were not global, because prenatal TBT exposure had no effect on the methylation status of at least one site on PPARγ2. This is in accordance with recent findings from Lillycrop *et al.* (63) showing that PPARα promoter region was demethylated in the offspring of rats fed a low-protein diet whereas PPARγ was not affected. It was proposed that two separate PPAR-dependent mechanisms might be involved in the fetal adaptations to the maternal diet. In this model, a PPARγ and PPARβ/δ mechanism regulates cell growth and differentiation, whereas another mechanism adapts long-term lipid metabolism via epigenetic changes in PPARα to optimize postnatal survival (17). This leads to the inference that TBT is likely to cause epigenetic modification of PPARγ target genes such as Fapb4 in MSCs, favoring their expression later in life and predisposing these cells to become adipocytes to the detriment of osteocytes. It will be of great interest to explore these mechanisms in future studies.

There is an urgent need to understand the molecular events underlying the predisposition to obesity and related disorders. There is increasing evidence from laboratories around the world to support an important role for environmental factors such as exposure to xenobiotic chemicals in the development of obesity. However, compared with diet and lifestyle, these environmental factors are understudied to date. Therefore, a detailed study of the role of environmental chemicals on the etiology of obesity, particularly via maternal exposure, is timely and important. This study showed that, as predicted from the obesogen hypothesis, TBT is involved in critical steps of adipogenesis *in vitro* and *in vivo*. Prenatal TBT exposure predisposes adipose-derived multipotent stem cells to become adipocytes at the expense of the osteoblast lineage. It remains to be determined whether TBT exposure or other *in vivo* cues might trigger the migration and the differentiation of these cells, or other MSCs (*e.g.* from the bone marrow) *in vivo*. It will be important for future studies to address the fate of MSCs from various locations in the body and determine whether circulating MSCs actually colonize fat depots during development and early adulthood. In addition, understanding how exposure to TBT and other obesogens may modulate a shift in the

commitment of MSCs from the osteogenic to the adipogenic lineages may provide important insight into understanding the link between obesity and bone loss that result from treatment with PPARγ activators.

Materials and Methods

Animals

Male and female C57BL/6J mice (8 wk of age) were purchased from The Jackson Laboratory (Bar Harbor, ME). Mice were housed in micro-isolator cages in a temperature-controlled room (22–24 C) with a 12-h light, 12-h dark cycle and provided water and food (standard low-fat diet for rodents RMH 2500; Purina Mills, Richmond, IN) *ad libitum*. All procedures conducted in this study were approved by the Institutional Animal Care and Use Committee of the University of California Irvine.

Chemical dosing

Unless otherwise specified, all chemicals were purchased from Sigma-Aldrich (St. Louis, MO). To identify a suitable TBT concentration to use in experiments, adult females were dosed by gavage feeding with TBT (0.01, 0.03, 0.1, 0.3, 3 or 10 mg/kg body weight). After 24 h, induction of the PPARγ target genes fatty acid synthase, fatty acid transport protein, acetyl-CoA-carboxylase, and sterol response element-binding protein 1c was measured by quantitative real-time RT-PCR (QPCR) as described below.

Fetal and neonatal exposure to TBT

Males and females were mated overnight, and females were checked for a copulation plug the following day (defined as d 0.5 of pregnancy). Pregnant females were dosed by gavage with TBT (0.1 mg/kg), ROSI (1 mg/kg) (Cayman Chemical, Ann Arbor, MI), or vehicle [0.5% carboxymethyl cellulose (CMC)] at E16.5. The exposed pups were kept with their dams and weaned at 20–22 d of age. Exposed mice were killed at 8 wk of age, and stromal stem cells were isolated from white epididymal/ovarian fat pads (WAT).

Cell models

For maintenance, all cells were grown as subconfluent monolayers in basic MSC expansion medium, which consisted of α-MEM without nucleosides (Invitrogen, Carlsbad, CA) supplemented with 16.5% FBS (Premium Select; Atlanta Biologicals, Atlanta, GA), 100 U/ml penicillin, 100 μg/ml streptomycin, 1 mM sodium pyruvate, and 4 mM L-glutamine. All cell types were plated at high density (10^5 cells/cm^2). Spontaneous differentiation was avoided using low (<6) passage cells that were prevented from becoming confluent.

hADSCs

hADSCs were purchased from Invitrogen (STEMPRO hADSCs). These ADSCs were isolated through mechanical and enzymatic digestion from cryopreserved human adipose tissue collected during liposuction procedures. Each lot contains passage 1 cells fully characterized by flow cytometry, with an expression profile consistent with an MSC population, and able to differentiate into adipocytes, osteoblasts, and chondrocytes.

mADSCs

Epididymal or ovarian fat pads from male (n = 5) or female (n = 5) mice that had been exposed to TBT, ROSI, or CMC (negative control) *in utero* were removed, washed with PBS, cut into small pieces, and then digested at 37 C for 1 h with 2 mg/ml collagenase type-I under gentle agitation. The digest was diluted with α-MEM-10% calf serum, and the suspension was centrifuged for 10 min at 260 × *g*. The pellet was resuspended and filtered through a 100 μm mesh to remove clumps. Cells were washed by a second centrifugation and seeded at high density.

In vivo and *ex vivo* effects of TBT on stem cell proliferation and differentiation capacities

Cells were treated with fat, bone or cartilage differentiation medium, or basic MSC expansion medium (untreated cells for no differentiation controls), for 14 or 21 d. Every 3 d, the medium was aspirated, cells were gently washed with PBS, and fresh medium was added. Differentiation medium was supplemented with DMSO (vehicle control), 5 and 50 nM TBT, or 500 nM ROSI (positive control for PPARγ2 induction). These TBT and ROSI concentrations are suitable to induce adipogenesis in the 3T3-L1 preadipocyte murine model and can activate adipocyte differentiation in hMSCs (data not shown). For the adipogenesis assay, additional treatment groups with 50 nM TTNPB (RAR agonist and negative control for differentiation) and 50 nM AGN (RXR agonist) (gift of Allergan Pharmaceuticals, Irvine, CA) were added. The effect of TBT exposure *in utero* was analyzed in cells harvested from adult animals, as previously described (19). Additional *in vitro* effects of TBT treatment were observed by the addition of TBT to the differentiation media of all cell types.

Adipose and bone differentiation

Media were prepared by adding the indicated components to basic MSC expansion medium. Standard adipogenic differentiation (MDII cocktail) was as follows: adipogenesis induction cocktail: 500 μM isobutylmethylxanthine (Toronto Research Chemical Inc., Toronto, Ontario, Canada), 1 μM dexamethasone, 200 μM indomethacin, and 5 μg/ml insulin. Adipose differentiation was also performed in the presence of the PPARγ antagonist T0070907 (Cayman, Chemical, Ann Harbor, MI). Osteogenic differentiation medium contained 50 μM L-ascorbic acid, 20 mM β-glycerol phosphate, and 10 nM dexamethasone. At the end of the induction period, cells were fixed in 10% buffered formalin for 20 min at room temperature and stained with Oil Red O for adipocytes or Alizarin Red S for osteoblasts. Three random fields from each well were photographed under phase contrast. For quantification of the number of cells containing lipid, cells were counter stained with 5 μg/ml Hoechst dye in PBS. Cells were visually counted. Lipid accumulation was quantified using Image J (version 1.36b; Wayne Rasband) as previously described (19). Data represent mean ± SEM from n = 3 wells per treatment and n = 3 pictures per well.

Cartilage differentiation

MSCs (2.5×10^5) were collected by centrifugation and grown as spheroids in wells containing cartilage differentiation medium [4.5 g/liter glucose DMEM, 50 mg/ml ITS premix, 50 μg/ml L-ascorbic acid-2-phosphate, 100 nM dexamethasone, 1.25 mg/ml BSA, 100 μg/ml sodium pyruvate, 40 μg/ml proline,

5.35 μg/ml linoleic acid, 2 mM l-glutamine, 10 ng/ml TGF-β3 (R&D Systems, Minneapolis, MN).

Proliferation assay

Cells were plated (n = 400) and expanded for 3, 9, and 12 d in basic MSC expansion media supplemented with DMSO vehicle control, MDII adipogenic induction cocktail, 50 nM TTNPB, 50 nM AGN, 10, 100, and 500 nM ROSI, and 1, 5, 10, 50, or 100 nM TBT. The density of cultured cells was assayed by DNA quantification using the CyQuant Cell Proliferation Assay Kit (Invitrogen) following manufacturer's instructions. A standard curve was prepared to quantity the cell number at the end of the assay. Results from all time points were averaged (n = 3 wells per treatment and per time point).

Analysis of mRNA by real-time PCR

Total RNA was extracted using the TRIzol reagent (Life Technologies, Gaithersburg, MD). The cDNA was generated from 1 μg DNase-treated RNA using SuperScript III RNase H$^-$ Reverse Transcriptase (Invitrogen) after DNase I digestion (Ambion, Austin, TX) following the manufacturer recommended protocol. Real-time PCR was performed in the DNA Engine Opticon Thermal Cycler [MJ Research (Watertown, MA)/Bio-Rad Laboratories (Hercules, CA)]. Quantitative PCR analyses for target genes (listing in Supplemental Table 1 published on The Endocrine Society's Journals Online web site at http://mend.endojournals.org) were performed with FastStart SYBR Green QPCR Master Mix (Roche, Nutley, NJ) and 100 nM of primers chosen with PerlPrimer (version 1.1.14; copyright 2003–2006, Owen Marshall). Primer sequences, annealing temperature, and amplicon size are presented in Supplemental Table 1. Relative quantification of the target gene transcript, in comparison with β-actin (housekeeping gene) expression level in the same sample, was made following the Pfaffl method (64). This method modifies the ΔΔCt approach by computing an expression ratio that accounts for differences in PCR efficiency among primer sets and uses the crossing point deviation of the unknown sample *vs.* the control group samples (untreated, DMSO, or CMC treatment, depending on the experiment). The ratio, representing the relative quantification of the target, is calculated as follows: $r = [(E_{target})^{\Delta CT_{target}(\text{mean control} - \text{mean unknown sample})}]/[(E_{\beta\text{-act}})^{\Delta CT_{\beta\text{-act}}(\text{mean control} - \text{mean unknown sample})}]$ (in which E is PCR efficiency determined by standard curve using serial dilution of cDNA; ΔCT is the crossing point deviation of an unknown sample *vs.* control.

Flow cytometry

Before any differentiation was induced, low-passage cultured ADSCs retrieved from mice exposed to CMC control or TBT *in utero* were harvested and washed with cold cytometry buffer (1% FBS, 4% sodium azide in PBS). Antimouse CD68 was purchased from Serotec (Oxford, UK), and antimouse aP2 and goat IgG isotype control were purchased from R&D Systems (Minneapolis, MN). Intracellular staining was performed using Fixation/Permeabilization solution according to the manufacturer's instructions (eBiosciences, San Diego, CA). The specificity of Fapb4 staining was assayed in 3T3-L1 cells. There is a 50% increase in the number of Fabp4-positive cells 48 h after induction (Supplemental Fig. 4). Cells were collected using FACSCalibur (Becton Dickinson, Franklin Lakes, NJ), and data were analyzed with FlowJo software (Treestar, Ashland, OR).

Methylation status of Fabp4 promoter/enhancer region

The Fabp4 (aP2) promoter/enhancer region examined (GenBank accession no. NT_078380.6) spanned 22 potentially methylated cytosines within nucleotides −1500 to +1000 with respect to the transcription start site and contains three restriction sites (Fapb4-Met1, Fapb4-Met2, and Fapb4-Met3) for the methylation-sensitive enzyme *Aci*I. The PPARγ2 promoter/enhancer region examined (GenBank accession no. NT_039353) spanned 11 potentially methylated cytosines within nucleotides −1500 to +1000 and contains one restriction site (PPARγ2-Met1) for the methylation-sensitive enzyme *Acl*I. Genomic DNA was isolated from undifferentiated mADSCs derived from animals exposed *in utero* to TBT or CMC by lysis in proteinase K (0.25 mg/ml) and sodium dodecyl sulfate 1% followed by phenol/chloroform/isoamyl alcohol extraction and ethanol precipitation. DNA (10 μg) was digested with excess *Aci*I or *Acl*I (New England Biolabs, Beverly, MA). The occurrence of methylation-sensitive digestion was assayed by QPCR with primers designed to span the three *Aci*I restriction sites for the study of the methylation status of Fapb4 promoter/enhancer region (Fapb4-Met1-F/R: ccttcagtcagtgtgggtttgc/ ggtggtgtcatcgggaaaatg; Fapb4-Met2-F/R: cacacacacacacacacaca/ gcattacttttattttggttctggta; and Fapb4-Met3-F/R: cagcgtaactcaccaccacca/ tgcccacagagcatcataacc), and primers designed to span the *Acl*I restriction site for the study of the methylation status of PPARγ2 (PPARγ2-Met1-F/R: cacgcccctcacagaacagt/ tgggaataaacacagaaagaatcagg). Other sets of primers (Fapb4-uncut-F/R: tcctctctgctgcccctctc/ gcctcttgtgccttgtgctg; and PPARγ2-uncut-F/R: cgttagcagtttggcacagc/ agccctccctgagaataatgt), designed to amplify a region containing no *Aci*I or *Acl*I restriction sites, were used as normalization controls. Relative quantification of Met fragments in comparison with the unchanged control (uncut), representing the methylation status of the promoter/enhancer regions, was calculated as followed: $r = [(E_{Met})^{\Delta CT_{Met}(\text{mean control} - \text{mean unknown sample})}]/[(E_{uncut})^{\Delta CT_{uncut}(\text{mean control} - \text{mean unknown sample})}]$.

Statistical analyses

Data are presented as means ± SEM. A Kruskal-Wallis nonparametric test, followed by a Dunn's *post hoc* test, were used to determine the significance of the difference in relative mRNA abundance or staining among groups with different treatments. $P < 0.05$ was considered statistically significant. Statistical analysis used the GraphPad Prism 5.0 (GraphPad Software, Inc., San Diego, CA).

Acknowledgments

We thank Drs. T. Iguchi, G. MacGregor, and members of the Blumberg laboratory for critical reading and comments on the manuscript and Dr. Roshantha Chandraratna (then at Allergan) for a gift of AGN). We also thank former UCI undergraduate student Starlynn Clarke for technical help in the execution of some experiments.

Address all correspondence and requests for reprints to: B. Blumberg, Department of Developmental and Cell Biology, 2011 Biological Sciences 3, University of California, Irvine, California 92697-2300. E-mail: blumberg@uci.edu.

This work was supported by National Institutes of Health Grant ES-015849 (to B.B.).

Disclosure Summary: S.K., T.K., C.C., and S.C. have nothing to declare. B.B. is a named inventor on U.S. patents US 5,861,274, US 6,200,802, and US 6,815,168 and US 7,250,273 related to PPARγ.

References

1. **Herbert A** 2008 The fat tail of obesity as told by the genome. Curr Opin Clin Nutr Metab Care 11:366–370
2. **Power C, Jefferis BJ** 2002 Fetal environment and subsequent obesity: a study of maternal smoking. Int J Epidemiol 31:413–419
3. **Mantena SK, King AL, Andringa KK, Eccleston HB, Bailey SM** 2008 Mitochondrial dysfunction and oxidative stress in the pathogenesis of alcohol- and obesity-induced fatty liver diseases. Free Radic Biol Med 44:1259–1272
4. **Hill JO, Peters JC** 1998 Environmental contributions to the obesity epidemic. Science 280:1371–1374
5. **Garruti G, Cotecchia S, Giampetruzzi F, Giorgino F, Giorgino R** 2008 Neuroendocrine deregulation of food intake, adipose tissue and the gastrointestinal system in obesity and metabolic syndrome. J Gastrointestin Liver Dis 17:193–198
6. **Rippe JM, Hess S** 1998 The role of physical activity in the prevention and management of obesity. J Am Diet Assoc 98:S31–S38
7. **Baillie-Hamilton PF** 2002 Chemical toxins: a hypothesis to explain the global obesity epidemic. J Altern Complement Med 8:185–192
8. **Heindel JJ** 2003 Endocrine disruptors and the obesity epidemic. Toxicol Sci 76:247–249
9. **Curhan GC, Willett WC, Rimm EB, Spiegelman D, Ascherio AL, Stampfer MJ** 1996 Birth weight and adult hypertension, diabetes mellitus, and obesity in US men. Circulation 94:3246–3250
10. **Barker DJ, Fall CH** 1993 Fetal and infant origins of cardiovascular disease. Arch Dis Child 68:797–799
11. **Bertram CE, Hanson MA** 2001 Animal models and programming of the metabolic syndrome. Br Med Bull 60:103–121
12. **Budge H, Gnanalingham MG, Gardner DS, Mostyn A, Stephenson T, Symonds ME** 2005 Maternal nutritional programming of fetal adipose tissue development: long-term consequences for later obesity. Birth Defects Res C Embryo Today 75:193–199
13. **Taylor PD, Poston L** 2007 Developmental programming of obesity in mammals. Exp Physiol 92:287–298
14. **Gluckman PD, Hanson MA, Beedle AS, Raubenheimer D** 2008 Fetal and neonatal pathways to obesity. Front Horm Res 36:61–72
15. **Mathers JC** 2007 Early nutrition: impact on epigenetics. Forum Nutr 60:42–48
16. **Mikkelsen TS, Hanna J, Zhang X, Ku M, Wernig M, Schorderet P, Bernstein BE, Jaenisch R, Lander ES, Meissner A** 2008 Dissecting direct reprogramming through integrative genomic analysis. Nature 454:49–55
17. **Rees WD, McNeil CJ, Maloney CA** 2008 The roles of PPARs in the fetal origins of metabolic health and disease. PPAR Res 2008: 459030
18. **Grün F, Blumberg B** 2007 Perturbed nuclear receptor signaling by environmental obesogens as emerging factors in the obesity crisis. Rev Endocr Metab Disord 8:161–171
19. **Grün F, Watanabe H, Zamanian Z, Maeda L, Arima K, Cubacha R, Gardiner DM, Kanno J, Iguchi T, Blumberg B** 2006 Endocrine-disrupting organotin compounds are potent inducers of adipogenesis in vertebrates. Mol Endocrinol 20:2141–2155
20. **Casals-Casas C, Feige JN, Desvergne B** 2008 Interference of pollutants with PPARs: endocrine disruption meets metabolism. Int J Obes (Lond) Suppl 6: S53–S61
21. **Grün F, Blumberg B** 2006 Environmental obesogens: organotins and endocrine disruption via nuclear receptor signaling. Endocrinology 147(Suppl 6):S50–S55
22. **Golub M, Doherty J** 2004 Triphenyltin as a potential human endocrine disruptor. J Toxicol Environ Health B Crit Rev 7:281–295
23. **Oberdörster E, McClellan-Green P** 2002 Mechanisms of imposex induction in the mud snail, *Ilyanassa obsoleta*: TBT as a neurotoxin and aromatase inhibitor. Mar Environ Res 54:715–718
24. **McAllister BG, Kime DE** 2003 Early life exposure to environmental levels of the aromatase inhibitor tributyltin causes masculinisation and irreversible sperm damage in zebrafish (*Danio rerio*). Aquat Toxicol 65:309–316
25. **Shimasaki Y, Kitano T, Oshima Y, Inoue S, Imada N, Honjo T** 2003 Tributyltin causes masculinization in fish. Environ Toxicol Chem 22:141–144
26. **Ogata R, Omura M, Shimasaki Y, Kubo K, Oshima Y, Aou S, Inoue N** 2001 Two-generation reproductive toxicity study of tributyltin chloride in female rats. J Toxicol Environ Health A 63:127–144
27. **Avram MM, Avram AS, James WD** 2007 Subcutaneous fat in normal and diseased states 3. Adipogenesis: from stem cell to fat cell. J Am Acad Dermatol 56:472–492
28. **Rosen ED, MacDougald OA** 2006 Adipocyte differentiation from the inside out. Nat Rev Mol Cell Biol 7:885–896
29. **Schäffler A, Büchler C** 2007 Concise review: adipose tissue-derived stromal cells—basic and clinical implications for novel cell-based therapies. Stem Cells 25:818–827
30. **Janderová L, McNeil M, Murrell AN, Mynatt RL, Smith SR** 2003 Human mesenchymal stem cells as an in vitro model for human adipogenesis. Obes Res 11:65–74
31. **Gimble JM, Robinson CE, Wu X, Kelly KA, Rodriguez BR, Kliewer SA, Lehmann JM, Morris DC** 1996 Peroxisome proliferator-activated receptor-γ activation by thiazolidinediones induces adipogenesis in bone marrow stromal cells. Mol Pharmacol 50:1087–1094
32. **Muruganandan S, Roman AA, Sinal CJ** 2009 Adipocyte differentiation of bone marrow-derived mesenchymal stem cells: cross talk with the osteoblastogenic program. Cell Mol Life Sci 66:236–253
33. **Peister A, Mellad JA, Larson BL, Hall BM, Gibson LF, Prockop DJ** 2004 Adult stem cells from bone marrow (MSCs) isolated from different strains of inbred mice vary in surface epitopes, rates of proliferation, and differentiation potential. Blood 103:1662–1668
34. **Burris TP, Pelton PD, Zhou L, Osborne MC, Cryan E, Demarest KT** 1999 A novel method for analysis of nuclear receptor function at natural promoters: peroxisome proliferator-activated receptor γ agonist actions on aP2 gene expression detected using branched DNA messenger RNA quantitation. Mol Endocrinol 13:410–417
35. **Ibrahimi A, Teboul L, Gaillard D, Amri EZ, Ailhaud G, Young P, Cawthorne MA, Grimaldi PA** 1994 Evidence for a common mechanism of action for fatty acids and thiazolidinedione antidiabetic agents on gene expression in preadipose cells. Mol Pharmacol 46: 1070–1076
36. **Sul HS, Smas C, Mei B, Zhou L** 2000 Function of pref-1 as an inhibitor of adipocyte differentiation. Int J Obes Relat Metab Disord 24(Suppl 4):S15–S19
37. **Gregoire FM** 2001 Adipocyte differentiation: from fibroblast to endocrine cell. Exp Biol Med (Maywood) 226:997–1002
38. **Quarto N, Longaker MT** 2006 FGF-2 inhibits osteogenesis in mouse adipose tissue-derived stromal cells and sustains their proliferative and osteogenic potential state. Tissue Eng 12:1405–1418
39. **Hasegawa T, Oizumi K, Yoshiko Y, Tanne K, Maeda N, Aubin JE** 2008 The PPARγ-selective ligand BRL-49653 differentially regulates the fate choices of rat calvaria versus rat bone marrow stromal cell populations. BMC Dev Biol 8:71
40. **Liu X, Zhou GD, Lü XJ, Liu TY, Zhang WJ, Liu W, Cao YL** 2007 [Potential of chondrogenesis of bone marrow stromal cells co-cultured with chondrocytes on biodegradable scaffold: in vivo experiment with pigs and mice]. Zhonghua Yi Xue Za Zhi 87:1929–1933
41. **Benvenuti S, Cellai I, Luciani P, Deledda C, Baglioni S, Giuliani C, Saccardi R, Mazzanti B, Dal Pozzo S, Mannucci E, Peri A, Serio M** 2007 Rosiglitazone stimulates adipogenesis and decreases osteo-

blastogenesis in human mesenchymal stem cells. J Endocrinol Invest 30:RC26–RC30
42. **Tchoukalova YD, Sarr MG, Jensen MD** 2004 Measuring committed preadipocytes in human adipose tissue from severely obese patients by using adipocyte fatty acid binding protein. Am J Physiol Regul Integr Comp Physiol 287:R1132–R1140
43. **Kanayama T, Kobayashi N, Mamiya S, Nakanishi T, Nishikawa J** 2005 Organotin compounds promote adipocyte differentiation as agonists of the peroxisome proliferator-activated receptor γ/retinoid X receptor pathway. Mol Pharmacol 67:766–774
44. **Chamberlain G, Fox J, Ashton B, Middleton J** 2007 Concise review: mesenchymal stem cells: their phenotype, differentiation capacity, immunological features, and potential for homing. Stem Cells 25: 2739–2749
45. **Carfi' M, Croera C, Ferrario D, Campi V, Bowe G, Pieters R, Gribaldo L** 2008 TBTC induces adipocyte differentiation in human bone marrow long term culture. Toxicology 249:11–18
46. **Crossno Jr JT, Majka SM, Grazia T, Gill RG, Klemm DJ** 2006 Rosiglitazone promotes development of a novel adipocyte population from bone marrow-derived circulating progenitor cells. J Clin Invest 116:3220–3228
47. **Koh YJ, Kang S, Lee HJ, Choi TS, Lee HS, Cho CH, Koh GY** 2007 Bone marrow-derived circulating progenitor cells fail to transdifferentiate into adipocytes in adult adipose tissues in mice. J Clin Invest 117:3684–3695
48. **Takahashi S, Mukai H, Tanabe S, Sakayama K, Miyazaki T, Masuno H** 1999 Butyltin residues in livers of humans and wild terrestrial mammals and in plastic products. Environ Pollut 106:213–218
49. **Kannan K, Grove RA, Senthilkumar K, Henny CJ, Giesy JP** 1999 Butyltin compounds in river otters (*Lutra canadensis*) from the northwestern United States. Arch Environ Contam Toxicol 36:462–468
50. **Nielsen JB, Strand J** 2002 Butyltin compounds in human liver. Environ Res 88:129–133
51. **Tsuda T, Inoue T, Kojima M, Aoki S** 1995 Daily intakes of tributyltin and triphenyltin compounds from meals. J AOAC Int 78: 941–943
52. **Otto TC, Lane MD** 2005 Adipose development: from stem cell to adipocyte. Crit Rev Biochem Mol Biol 40:229–242
53. **Farmer SR** 2005 Regulation of PPARγ activity during adipogenesis. Int J Obes (Lond) 29(Suppl 1):S13–S16
54. **Walkey CJ, Spiegelman BM** 2008 A functional peroxisome proliferator-activated receptor-gamma ligand-binding domain is not required for adipogenesis. J Biol Chem 283:24290–24294
55. **Yang W, Rachez C, Freedman LP** 2000 Discrete roles for peroxisome proliferator-activated receptor γ and retinoid X receptor in recruiting nuclear receptor coactivators. Mol Cell Biol 20:8008–8017
56. **Aubin JE** 1998 Bone stem cells. J Cell Biochem (Suppl 30–31): 73–82
57. **Song L, Tuan RS** 2004 Transdifferentiation potential of human mesenchymal stem cells derived from bone marrow. FASEB J 18: 980–982
58. **Akune T, Ohba S, Kamekura S, Yamaguchi M, Chung UI, Kubota N, Terauchi Y, Harada Y, Azuma Y, Nakamura K, Kadowaki T, Kawaguchi H** 2004 PPARγ insufficiency enhances osteogenesis through osteoblast formation from bone marrow progenitors. J Clin Invest 113:846–855
59. **Post S, Abdallah BM, Bentzon JF, Kassem M** 2008 Demonstration of the presence of independent pre-osteoblastic and pre-adipocytic cell populations in bone marrow-derived mesenchymal stem cells. Bone 43:32–39
60. **Vickers MH** 2007 Developmental programming and adult obesity: the role of leptin. Curr Opin Endocrinol Diabetes Obes 14:17–22
61. **Prestwich TC, Macdougald OA** 2007 Wnt/β-catenin signaling in adipogenesis and metabolism. Curr Opin Cell Biol 19:612–617
62. **Takada I, Mihara M, Suzawa M, Ohtake F, Kobayashi S, Igarashi M, Youn MY, Takeyama K, Nakamura T, Mezaki Y, Takezawa S, Yogiashi Y, Kitagawa H, Yamada G, Takada S, Minami Y, Shibuya H, Matsumoto K, Kato S** 2007 A histone lysine methyltransferase activated by non-canonical Wnt signalling suppresses PPAR-γ transactivation. Nat Cell Biol 9:1273–1285
63. **Lillycrop KA, Phillips ES, Jackson AA, Hanson MA, Burdge GC** 2005 Dietary protein restriction of pregnant rats induces and folic acid supplementation prevents epigenetic modification of hepatic gene expression in the offspring. J Nutr 135:1382–1386
64. **Pfaffl MW** 2001 A new mathematical model for relative quantification in real-time RT-PCR. Nucleic Acids Res 29:e45